

# Measurements of Electron Density in the Charge Exchange Plasma of an Ion Thruster

P. C. T. de Boer\*

*The Aerospace Corporation, Los Angeles, California 90009-2957*

The electron density in the charge exchange plasma emitted by a xenon ion thruster is determined using a langmuir probe. It is shown that the electron density in this plasma is sufficiently low to allow the use of orbital-motion-limited theory. In applying this theory, the inflection point in the experimental current–voltage characteristic is taken as the point where the probe voltage equals the plasma potential. The electron density then follows from letting the theoretical result for the characteristic coincide with the experimental one at a significantly larger voltage. Satisfactory agreement is obtained between theoretical and experimental curves. The results obtained for the electron density are compared with corresponding results for the ion density, determined from the ion saturation current. The ion density measurements are valid in the main ion beam, but not in the charge exchange plasma. The electron density measurements are valid in the charge exchange plasma and in the downstream part of the ion beam, but not in its upstream part. In the regions where both results are valid, they agree within experimental accuracy. The composite result covers charged particle densities over the range  $10^8$ – $10^{10}$  cm $^{-3}$ .

## Nomenclature

$A$	= area, m $^2$
$D$	= probe diameter, $1 \pm 0.02$ mm
$e$	= electron charge, $1.602 \times 10^{-19}$ C
$J$	= current, A
$k$	= Boltzmann constant, $1.380 \times 10^{-23}$ J/K
$L$	= probe length, $12 \pm 0.1$ mm
$m$	= mass, kg
$n$	= number density, m $^{-3}$
$r$	= radius, m
$T$	= temperature, K
$u_i$	= ion velocity, m/s
$V$	= electric potential, V
$\Delta V$	= beam voltage, $1100 \pm 10$ V
$\epsilon_0$	= dielectric constant for vacuum, $8.854 \times 10^{-12}$ F/m
$\eta$	= $e(V_p - V_{pl})/(kT_e)$ , nondimensional probe potential
$\lambda_D$	= $(\epsilon_0 kT_e / n_e e^2)^{1/2}$ , Debye length, m
$\xi$	= $r/\lambda_D$

## Subscripts

$e$	= electron
$i$	= ion
$p$	= probe
$pl$	= plasma

## I. Introduction

ION thrusters have shown promise for use in geostationary satellites and in other space flight systems. The electrical power required can be obtained from solar radiation. Because of the large exit velocity of the ions emitted, only a relatively small propellant flow rate is required to achieve a given thrust. This is an important advantage in spacecraft design, which can be translated into either an extended lifetime, a larger payload, a lower cost, or a combination of these factors.

In addition to high-velocity ions, the thruster also emits low-velocity neutral atoms. Such atoms are subject to charge exchange collisions with the ions, resulting in a fast neutral atom and a low velocity ion. The motion of the resulting ion is governed to a large extent by the electric field in the ion beam. Close to the acceleration grids, the electric field will cause these ions to return to the thruster, where they cause harmful erosion of grids. Further downstream and away from the beam axis, the electric field has an appreciable radial component. As a result, there is a radial outflow of charge-exchange ions. These ions are accompanied by electrons, with the resulting electron density being nearly equal to the ion density. Absence of this so-called charge neutrality would set up electric fields leading to restoration of the neutrality. The resulting plasma, called the charge exchange plasma, is an undesirable byproduct that poses a possible contamination and erosion threat to solar panels and satellite instrumentation.<sup>1–3</sup> Therefore, it is important to study this plasma and to understand its behavior.

Previous studies of the charge exchange plasma were carried out by Carruth and Brady,<sup>4</sup> Carruth,<sup>5</sup> and Carruth et al.<sup>6</sup> These investigators exploited the end effect of a long, cylindrical langmuir probe to determine the flow direction of the charge exchange plasma at various locations. The ion current collected by the probe as a function of probe orientation allowed determination of the ion density and the plasma flow velocity. The results reported in Ref. 6 agree quite well with data obtained using a retarding potential analyzer or Faraday cup. It was found that part of the charge exchange plasma flows upstream of the ion thruster, indicating that contamination of the spacecraft's outer surfaces is of real concern.

Recent investigations of the plasma emitted by an ion thruster have made use of double and single electric probes.<sup>7,8</sup> The ion flux in the main ion beam could be determined from the saturation current. Because the velocity of the ions is known with good accuracy, this provides a measurement of the ion density in the beam. Measurements of the floating potential of a single probe indicated that the electric fields in the ion beam are relatively small, and that the degree of nonneutralization is only of order  $10^{-4}$ – $10^{-5}$ . Measurements of the ion flux were also obtained in the charge exchange plasma. However, because the velocity of the ions in this plasma is unknown, only a crude estimate could be made of the corresponding ion density.

In this paper, the experimental results of Ref. 7 obtained in the charge exchange plasma are further analyzed. It is shown that the current–voltage characteristics obtained in this region

Received April 18, 1996; revision received April 12, 1997; accepted for publication June 9, 1997. Copyright © 1997 by P. C. T. de Boer. Published by the American Institute of Aeronautics and Astronautics, Inc., with permission.

\*Research Physicist, Mechanics and Propulsion Department, P.O. Box 92957; currently Professor, Sibley School of Mechanical and Aerospace Engineering, Upson Hall, Cornell University, Ithaca, NY 14853. Associate Fellow AIAA.

lend themselves to application of langmuir's analytical results for the so-called thick sheath limit. In this limit, the current to the probe at large positive voltages is limited by orbital motion of the incoming electrons. The analytical results provide a current-voltage characteristic that can be fitted to the experimental result. The fit is based on letting the two results coincide at the voltage corresponding to the plasma potential as well as at a significantly larger voltage. This procedure fixes the electron density. Details of the procedure that was followed are given in Sec. III.

## II. Experimental Details

A sketch of the electric probe used is shown in Fig. 1. The probe was placed in the ion beam (plume) of a UK-10 xenon ion thruster.<sup>9-11</sup> This thruster is of the Kaufman type. It has 10-cm-diam twin grids that are dished inward. The diameter of the resulting ion beam initially decreases with increasing distance from the grids, but eventually increases because of beam spreading. The waist or narrowest part of the beam occurs about 15 cm from the grids. The beam divergence far from the thruster is  $11 \pm 10$  deg (Ref. 9). The thruster was run at conditions providing a nominal thrust of 18 mN: beam current  $0.33 \pm 0.01$  A, beam voltage  $\Delta V = 1100 \pm 10$  V, anode current  $2 \pm 0.02$  A, cathode keeper current  $1 \pm 0.01$  A, neutralizer keeper current  $0.66 \pm 0.01$  A, magnet current  $160 \pm 2$  mA, accelerator grid current  $1.5 \pm 0.02$  mA, accelerator grid voltage  $-340 \pm 5$  V, main xenon flow rate  $0.62 \pm 0.01$  mg/s, cathode xenon flow rate  $0.110 \pm 0.02$  mg/s, neutralizer xenon flow rate  $0.036 \pm 0.002$  mg/s. The neutralizer was kept at ground potential. The experiments were carried out in a vacuum chamber having a diameter of 2.4 m and a length of 5.5 m. The ion beam ended up at a grounded beam dump about 2.2 m from the thruster. The vacuum in the chamber was maintained by two CVI Torrmaster TM1200 cryopumps, supported by a Leyboldt TMP/NT 150/360V/H turbomolecular pump. During the experiments, most of the background gas was xenon at a pressure of about  $2 \pm 1 \times 10^{-6}$  torr ( $0.3 \pm 15$  mPa). This pressure was measured with an ionization gauge, using the xenon/air correction factor of 0.33. The electric probe was mounted on a Compumotor Model 4000 Positioning System. The axis of the probe was perpendicular to the axis of the ion beam. Both axes were in a horizontal plane. Probe traverses in this plane were made at distances of 5, 7.5, 10, 15, 25, 35, 48, and  $60 \pm 0.05$  cm, respectively, from the thruster grid. The center of the neutralizer was located  $6.2 \pm 0.1$  cm below the plane. Its horizontal distance from the beam center was  $-5.7 \pm 0.1$  cm, using the sign convention adopted in the figures shown in the next section. During each probe traverse, current-voltage ( $J$ - $V$ ) characteristics were taken at points  $0.64 \pm 0.01$  cm apart. To this purpose, the voltage on the probe was varied from 0 to 15 V with respect to ground, with increments of  $0.25 \pm 0.003$  V. The voltages were provided by a Kepco Model BOP100-1M bipolar operational power supply/amplifier. At each datum point, the current was measured 500 ms after the voltage was applied; this delay was sufficient to let transient effects die out. The current measurement followed from the voltage drop across a  $1.00 \pm 0.01$  k $\Omega$  resistance in series with the probe. This voltage drop was recorded using a Fluke model 8840A multimeter. A second Fluke 8840A provided an accurate record of the probe voltage. All measurements were taken with a computerized data acquisition system.

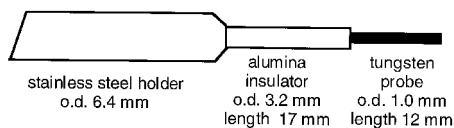


Fig. 1 Sketch of probe used.

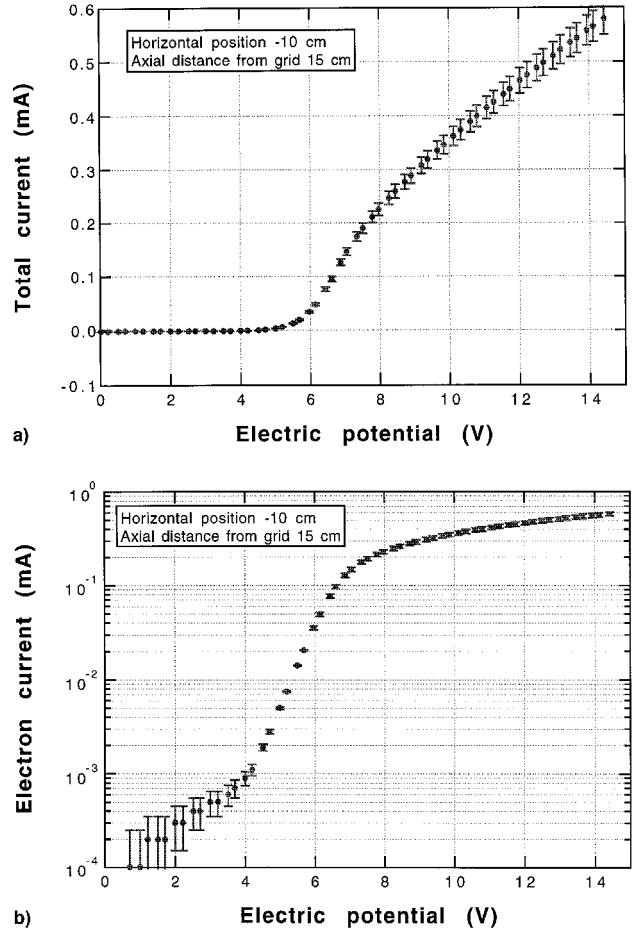


Fig. 2 Representative current-voltage characteristic obtained in the charge-exchange plasma: a) linear plot and b) semilogarithmic plot.

## III. Interpretation of Electric Probe Data

A representative  $J$ - $V$  characteristic obtained in the charge-exchange plasma is shown in Fig. 2a, which is identical to Fig. 17 of Ref. 3. The  $J$ - $V$  characteristics were found to be highly reproducible. The estimated inaccuracy in  $J$  is  $\pm 5\%$ , except at the lowest values, where it is  $\pm 1.5 \times 10^{-4}$  mA because of scale fineness. The same result is plotted in Fig. 2b using a logarithmic scale for the current. The interpretation of  $J$ - $V$  characteristics of this type is discussed in detail by Chen<sup>12</sup> and Chung et al.<sup>13</sup> For present purposes, principal interest is in the regime of large positive probe potentials  $V$ . The current in this regime is carried almost entirely by electrons. As a result of the space charge density of the electrons, the electric field around the probe is appreciable only over a finite region, called the sheath. If the sheath is thin compared with the probe radius, the current is limited by space charge effects. If the sheath is thick, the current is limited by the effects of orbital motion. Important parameters for determination of the regime in which a probe operates are the ratio of probe diameter to Debye length  $\xi_p$ , and the nondimensional probe potential  $\eta$ . For sufficiently small  $\xi_p$  and  $\eta$ , the current to a cylindrical probe is given by the classical orbital-motion-limited result<sup>12,14-16</sup>

$$J = eA_p n_e \frac{1}{4} \sqrt{\frac{8kT_e}{\pi m_e}} F(\eta) \quad (1)$$

with

$$F(\eta) = \frac{2}{\sqrt{\pi}} \eta^{1/2} + e^\eta [1 - \text{erf}(\sqrt{\eta})] \quad (2)$$

$$\eta = \frac{e(V_p - V_{pl})}{kT_e} \quad (3)$$

This result is useful for cases with relatively low electron density.<sup>12</sup> The charge exchange plasma appears to be such a case. This follows from comparing the detailed numerical results of Laframboise<sup>15</sup> with estimates of the relevant plasma parameters. For a typical case considered,  $n_e \approx 10^8 \text{ cm}^{-3}$ ,  $T_e \approx 0.5 \text{ eV}$ , yielding  $\lambda_D \approx 0.5 \text{ mm}$ . It follows that the ratio  $r_p/\lambda_D \approx 1$ . For  $\eta$  in the 5–15 range, the probe performance is well within the regime represented by Eqs. (1–3) (cf., Fig. 42 of Ref. 15). The applicability of Eqs. (1–3) is also illustrated by the goodness of fit with the experimental results.

In fitting a curve represented by Eqs. (1–3) to the  $J$ - $V$  characteristic obtained experimentally in the region of large  $V_p$  values must be determined for the three parameters  $T_e$ ,  $n_e$ , and  $V_{pl}$ . Use was made of a well-known model for the  $J$ - $V$  characteristic. This model separates the characteristic into an electron-retarding regime ( $V_p < V_{pl}$ ) and an electron-attracting regime ( $V_p > V_{pl}$ ). The electron-retarding potential in the region where  $V_p$  is less than  $V_{pl}$  causes a positive curvature of the characteristic. For  $V_p > V_{pl}$ , space-charge and orbital motion limitations cause the curvature to be negative. Therefore, the value of the plasma potential  $V_{pl}$  was chosen as the value of  $V_p$  at the point pl, where the curvature of the  $J$ - $V$  characteristic changes from positive to negative. This point was determined by computing the slopes of the straight line segments connecting successive  $J$ - $V$  measurements, and then finding the segment with the maximum slope. The point pl was taken at the middle of this segment. The noise in the data was quite low, and the determination of  $V_{pl}$  is estimated to be accurate within the voltage difference between data points (0.25 V). At the point pl,  $\eta = 0$  and  $F(\eta) = 1$ , whereas the current  $J$  to the probe equals the current  $J_{pl}$  caused by the thermal flux of electrons in the unperturbed plasma. The curve described by Eqs. (1–3) is also made to pass through a point  $q$  of the characteristic corresponding to a significantly larger voltage  $V_q$ . Whenever the available data allowed, this point was taken nominally 5 V (20 data points) beyond the point pl. If the data extended less than 5 V beyond pl, the point  $q$  was taken at the largest available value of  $V_p$ . The value of  $\eta_q$  followed by setting  $F$  in Eq. (2) equal to  $J_q/J_{pl}$  and by solving Eq. (2) for  $\eta$ . Next, the electron temperature was found from the relation  $kT_e/e = (V_q - V_{pl})/\eta_q$ , after which the electron density followed from Eq. (1), with  $J = J_{pl}$  and  $F = 1$ . In very few cases, all of which occurred at locations within the main ion beam, the points  $q$  and pl determined this way were found to coincide. No data were evaluated for such cases.

Representative examples of the resulting  $J$  vs  $V_p$  curves, together with the corresponding experimental results, are shown in Fig. 3. At the largest values of  $V_p$ , the experimental values of the current  $J$  tend to be somewhat larger than the results given by Eqs. (1–3). This is ascribed to end effects that arise when the sheath no longer is thin compared with the length of the probe. Apart from this tendency, the agreement between experimental results and results given by orbital-motion-limited theory was satisfactory. The procedure followed appears to yield reasonably accurate values ( $\pm 20\%$  or better) for  $n_e$  in the charge-exchange plasma and in the downstream part of the main ion beam, as illustrated in the next section.

The function  $F(\eta)$  can be represented by the asymptotic expansion

$$F(\eta) = \frac{2}{\sqrt{\pi}} \eta^{1/2} \left[ 1 + \frac{1}{2\eta} - \frac{1}{4\eta^2} + \mathcal{O}\left(\frac{1}{\eta^3}\right) \right] \quad (4)$$

Substituting this in Eq. (1) and solving for  $n_e$  yields

$$n_e = \pi \frac{J_q}{eA_p} \sqrt{\frac{m_e}{2e(V_q - V_{pl})}} \left/ \left[ 1 + \frac{1}{2\eta_q} - \frac{1}{4\eta_q^2} + \mathcal{O}\left(\frac{1}{\eta_q^3}\right) \right] \right. \quad (5)$$

This result involves  $T_e$  only through  $\eta_q \equiv e(V_q - V_{pl})/(kT_e)$ . Because  $kT_e$  in the charge exchange plasma is on the order of 0.5 eV (see Ref. 7),  $1/(2\eta_q)$  is on the order of 0.05. This indicates that the determination of  $n_e$  is insensitive to the precise value of  $T_e$ . This is fortunate, because inaccuracies in the measured ratio  $J_q/J_{pl}$  are enhanced in the value obtained for  $kT_e$ . The latter value is roughly proportional to  $(J_{pl}/J_q)^2$ , as can be seen by substituting the leading term of Eq. (4) into Eq. (1). The resulting inaccuracies in  $kT_e$  can be rather large ( $\pm 25\%$ ).

The ion density inside the main ion beam was determined from the measured ion saturation current  $J_s$ , using

$$n_i = J_s/(eu_i DL) \quad (6)$$

where  $u_i$  was taken to be  $(2e\Delta V/m_i)^{1/2} = 40 \pm 1 \text{ km/s}$ . This

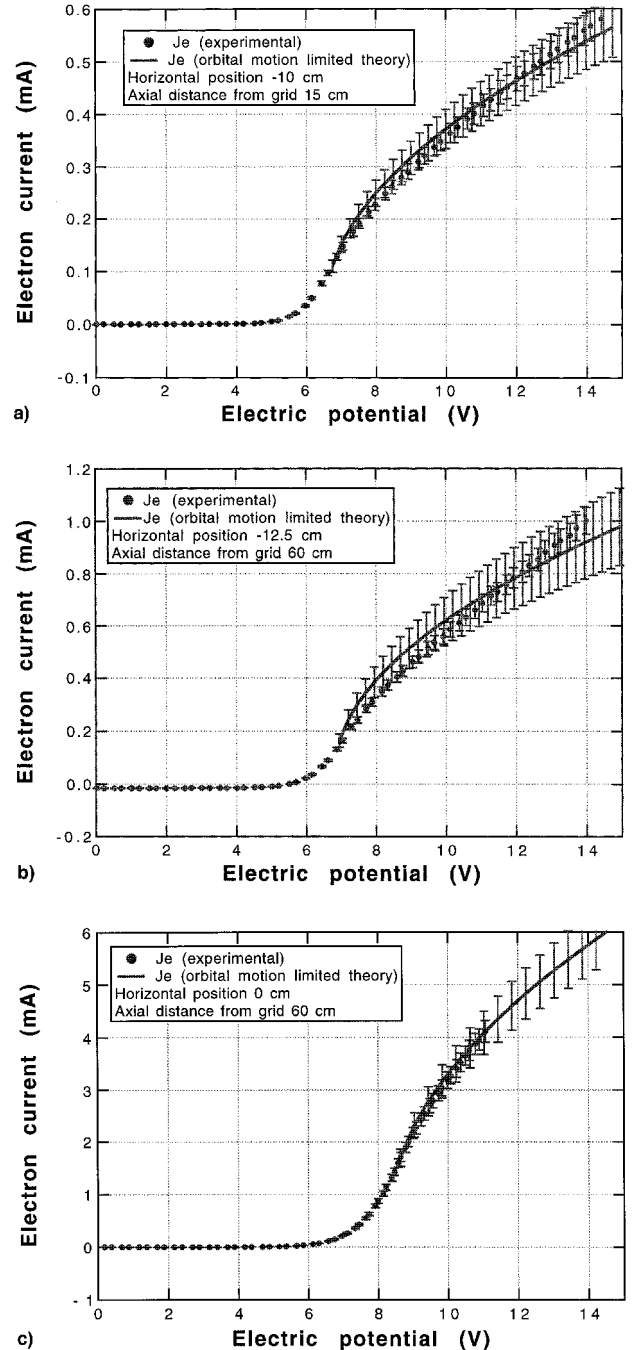


Fig. 3 Representative orbital-motion-limited theoretical results and corresponding experimental data: a) charge exchange plasma, 15 cm from grid; b) outer region of main beam, 60 cm from grid; and c) center of main beam, 60 cm from grid.

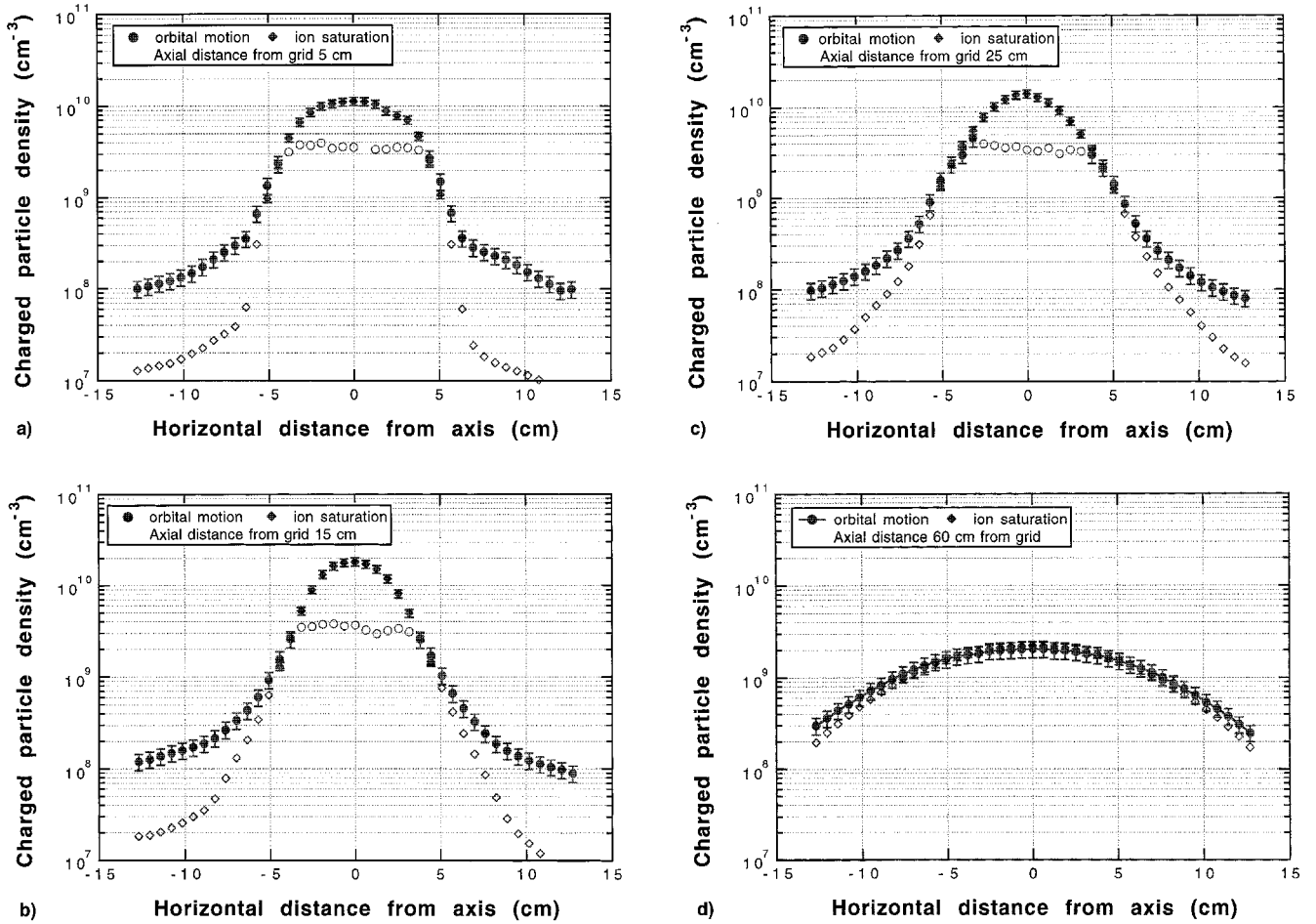


Fig. 4 Results for electron density from orbital-motion-limited theory, and for ion density determined from ion saturation current, at various distances from grid: a) 5, b) 15, c) 25, and d) 60 cm. Open symbols represent results for which the underlying theory is invalid.

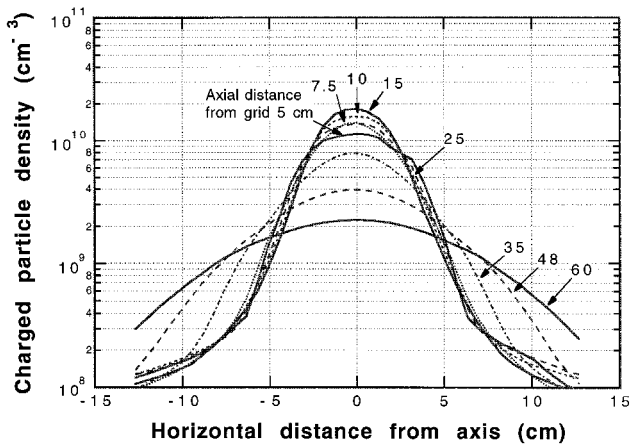


Fig. 5 Composite results for charged particle density.

equation is based on the following assumptions: 1) the ion paths are not perturbed before striking the probe, 2) the area of the probe projected on a plane perpendicular to the direction of the beam is  $DL$ , 3) secondary emission is negligible, and 4) all ions collected are singly charged. Because the ion energy is 1100 V while the probe potential is no larger than 15 V, the error arising from the first assumption is estimated to be no larger than 2%. When the probe is at its extreme off-axis position while 60 cm from the thruster, the projected area actually is about  $\cos[\tan^{-1}(12.5/60)]DL = 0.98 DL$ . This position is near the edge of the ion beam, and the resulting misalignment error of 2% is believed to not be exceeded in any other measure-

ments taken in the main ion beam. The error caused by the secondary emission is estimated to be 2% (Ref. 7), whereas the fraction of ions that is doubly charged is on the order of 3% (Ref. 9). Based on these errors, some of which tend to compensate each other, the total error in the results for the ion density is estimated to be on the order of  $\pm 10\%$ .

#### IV. Results Obtained

Using the method described in the previous section, the electron density was evaluated at each of the traverses. Results for the traverses at axial distances of 5, 15, 25, and 60 cm from the grid are shown in Fig. 4. Also shown are corresponding results for the ion density obtained from the ion saturation current. At 60 cm from the grid (Fig. 4d), both measurements produce valid results over most of the traverse. The ion saturation current collected consists primarily of ions in the main beam, having a directed velocity corresponding to 1100 eV. The electron density is sufficiently small to allow application of the method described in the previous section. At distances of 25 cm and less, this is no longer the case. Outside the main ion beam, the ion saturation current consists mainly of charge exchange ions, which have a velocity much lower than the velocity corresponding to 1100 V. This invalidates the method used for the determination of ion density. Inside the ion beam, the electron density is too high to allow application of orbital-motion-limited theory. Orbital-motion-limited theory is still applicable in the region outside the beam, and determination of ion density from ion current collected is still applicable inside the beam. Fortunately, as can be seen in Figs. 4a–4c, there is an intermediate region where the two sets of results agree. This indicates that the charged particle density over the entire tra-

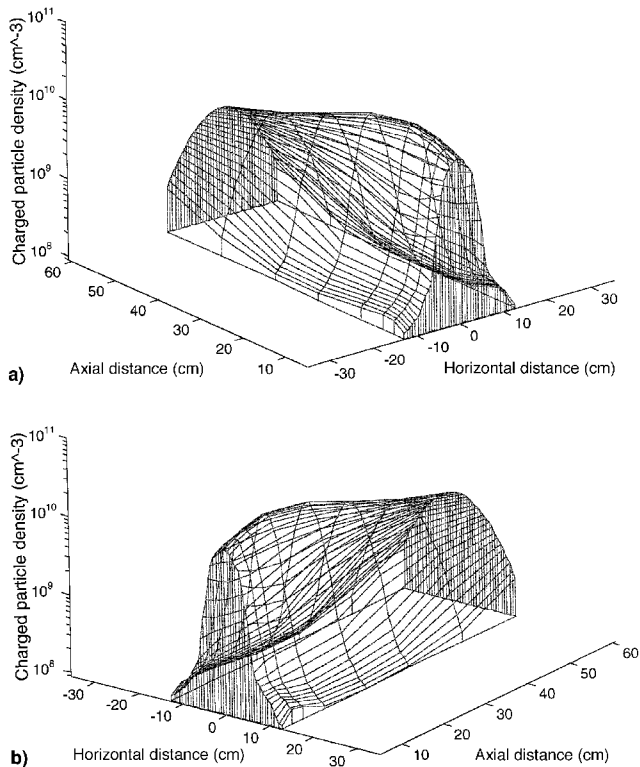


Fig. 6 Three-dimensional representation of composite results for charged particle density, viewed from different sides.

verse can be obtained as a composite of the two sets of results. The composite is obtained by taking the larger of the orbital-motion-limited result or the ion saturation result at each location (closed symbols). The open symbols represent results obtained under conditions where the underlying theory is invalid. Results for the composite are shown in two-dimensional form in Fig. 5, and in three-dimensional form in Figs. 6a and 6b. For a given horizontal distance, i.e., radius, from the axis, e.g.,  $-12.5$  cm, the charge exchange plasma appears to have a maximum density between 5–10 cm from the grid. At this horizontal distance, the density decreases gradually until an axial distance of about 35 cm. Beyond this point, the main ion beam has spread out to cause the density to increase markedly with axial distance. At each radial traverse, the density of the charge exchange plasma decreases markedly with horizontal distance from the axis, i.e., with radius.

Work along the lines described here was also carried out by Pollard.<sup>8</sup> His procedure consisted of using a piecewise function encompassing both the electron retarding region and the electron attracting region. The least-mean-squares fit to the data used  $V_{pl}$ ,  $T_e$ ,  $n_e$ , as well as the ratio of the sheath radius to the probe radius as fitting parameters. The lowest electron densities measured were on the order of  $5 \times 10^7$  cm<sup>-3</sup>. Pollard found that the data could be better fitted to the analytical result for a spherical probe than to that of a cylindrical probe. Presumably, this came about because the sheath radius was no longer small compared with the length of the probe, causing end effects to become important. The possible influence of end effects was also noted in Sec. III of this paper when discussing Figs. 3. As suggested by Pollard,<sup>7</sup> it may be preferable to use a spherical probe rather than a cylindrical one for measurements in the charge exchange plasma. Unfortunately, it is known that the largest allowed value of  $\xi_p$  for validity of orbital-motion-limited theory is much smaller for a spherical probe than for a cylindrical one.<sup>15</sup> The radius of a spherical probe used for this purpose therefore tends to be unacceptably small. Because of this, Laframboise and Parker<sup>16</sup> suggested the use of special probe geometries that yield the behavior of a spherical probe while still satisfying the criteria for validity of

orbital-motion-limited theory. The use of such special geometries appears to be an attractive possibility for the study of charge exchange plasmas.

## V. Concluding Remarks

The results reported in this paper indicate that it is possible to determine the electron density in the charge exchange plasma of a xenon ion thruster using a cylindrical electric probe and applying orbital-motion-limited theory. For typical conditions in this plasma, the ratio  $\xi_p$  of probe diameter to Debye length and the dimensionless probe potential  $\eta$  can be chosen such that the classical orbital-motion-limited results given by Eqs. (1–3) are applicable. Criteria for the corresponding magnitudes of  $\xi_p$  and  $\eta$  are given in Ref. 15. The applicability of Eqs. (1–3) was verified by computing the corresponding current–voltage characteristics, and by comparing these with experimental results. The theoretical characteristics were based on the premise that the plasma potential  $V_{pl}$  is equal to the probe voltage at the inflection point of the current–voltage characteristic, i.e., at the point where the characteristic achieves its maximum slope. The theoretical results were made to agree with the corresponding experimental ones at  $V_{pl}$  as well as at a potential  $V_q$  about 5 V larger than  $V_{pl}$ . The overall agreement between theoretical and experimental curves was within estimated accuracies. Inaccuracies in the theoretical results are believed to be caused mainly by end effects, which were not taken into account.

One of the principal questions regarding the charge exchange plasma concerns the motion of the ions, and the resulting potential of contamination of solar panels and satellite instruments. Further insight into this potential can be obtained by making measurements at locations not included in the present work. It will also be useful to carry out detailed numerical studies of the ion motion. Experimental results like the present ones can be helpful in verifying the accuracy of such studies.

## Acknowledgments

This work was sponsored by the Aerospace Sponsored Research program. The author thanks R. B. Cohen, M. W. Crofton, E. W. Fournier, S. W. Janson, L. K. Johnson, and J. E. Pollard of The Aerospace Corporation, and D. G. Fearn and N. Wallace of the U.K.'s Defence Research Agency (Farnborough) for help with various aspects of this work.

## References

- <sup>1</sup>Kaufman, H. R., "Charge-Exchange Plasma Generated by an Ion Thruster," NASA CR-134844, June 1975.
- <sup>2</sup>Kaufman, H. R., "Charge-Exchange Plasma Generated by an Ion Thruster," NASA CR-135318, Dec. 1977.
- <sup>3</sup>Byers, D. C., "Electron Bombardment Thruster Field and Particle Interfaces," *Journal of Spacecraft and Rockets*, Vol. 16, No. 5, 1979, pp. 289–301.
- <sup>4</sup>Carruth, M. R., Jr., and Brady, M. E., "Measurement of the Charge-Exchange Plasma Flow from an Ion Thruster," *Journal of Spacecraft and Rockets*, Vol. 18, No. 5, 1981, pp. 457–461.
- <sup>5</sup>Carruth, M. R., Jr., "A Review of Studies on Ion Thruster Beam and Charge-Exchange Plasmas," AIAA Paper 82-1944, Nov. 1982.
- <sup>6</sup>Carruth, M. R., Jr., Gabriel, S. B., and Kitamura, S., "Ion Thruster Charge-Exchange Plasma Flow," *Journal of Spacecraft and Rockets*, Vol. 19, No. 6, 1982, pp. 571–578.
- <sup>7</sup>de Boer, P. C. T., "Electric Probe Measurements in the Plume of the UK-10 Ion Thruster," *Journal of Propulsion and Power*, Vol. 12, No. 1, 1996, pp. 95–104.
- <sup>8</sup>Pollard, J. E., "Plume Angular, Energy, and Mass Spectral Measurements with the T5 Ion Engine," AIAA Paper 95-2920, July 1995.
- <sup>9</sup>Fearn, D. G., Martin, A. R., and Smith, P., "Ion Propulsion Research and Development in the UK," *Journal of British Interplanetary Society*, Vol. 43, No. 10, 1990, pp. 431–442.
- <sup>10</sup>Fearn, D. G., "The Control Philosophy of the UK-10 and UK-25 Ion Thrusters," AIAA Paper 90-2629, July 1990.

<sup>11</sup>Harvey, M. S., and the Staff of Space Applications Department, "The Advanced Propulsion Space Test Facilities at AEA Technology Culham Laboratory," 22nd International Electric Propulsion Conf., Paper 91-153, AEA Technology, Culham Lab., Abingdon, Oxon, UK, 1991.

<sup>12</sup>Chen, F. F., *Plasma Diagnostic Techniques*, edited by R. H. Huddleston and S. L. Leonard, Academic, New York, 1965.

<sup>13</sup>Chung, P. M., Talbot, L., and Touryan, K. J., *Electric Probes in Stationary and Flowing Plasmas: Theory and Application*, Springer-Verlag, New York, 1975.

<sup>14</sup>Langmuir, I., and Mott-Smith, H. M., *The Collected Works of Irving Langmuir*, edited by G. Suits, Vol. 4, Pergamon, New York, 1961, pp. 99-132.

<sup>15</sup>Laframboise, J. G., "Theory of Spherical and Cylindrical Langmuir probes in a Collisionless, Maxwellian Plasma at Rest," Inst. for Aerospace Studies, Univ. of Toronto, UTIAS Rept. 100, Toronto, ON, Canada, June 1966.

<sup>16</sup>Laframboise, J. G., and Parker, L. W., "Probe Design for Orbit-Limited Current Collection," *Physics of Fluids*, Vol. 16, No. 5, 1973, pp. 629-636.